International Journal of Pharmaceutics: X 2 (2020) 100053

Contents lists available at ScienceDirect

International Journal of Pharmaceutics: X

journal homepage: www.journals.elsevier.com/international-journal-of-pharmaceutics-x

Xyloglucan based mucosal nanovaccine for immunological protection against brucellosis developed by supercritical fluid technology

Swati Vyas, Sagar Dhoble[1], Vinod Ghodake[1], V. Patravale*

Department of Pharmaceutical Sciences and Technology, Institute of Chemical Technology, Matunga (E), Mumbai 400019, India

ARTICLE INFO

Keywords:
Brucellosis
Antigenic nanoparticles
Nanovaccine
Supercritical fluid
Xyloglucan

ABSTRACT

Vaccines delivered via the mucosal route have logistic benefits over parenteral or intramuscular vaccines as they offer patient compliance. This study presents the first intranasal, controlled release, subunit nanovaccine comprising mucoadhesive tamarind seed polymer (xyloglucan) based nanoparticles produced using an efficient, environmentally compatible, and industrially scalable technique: rapid expansion of supercritical solution. The nanovaccine formulation aimed against brucellosis comprised xyloglucan nanoparticles loaded separately with antigenic acellular lipopolysaccharides from *B. abortus* (S19) and the immunoadjuvant quillaja saponin. The nanovaccine elicited prolonged humoral and cell-mediated immunity in female Balb/c mice. Nasal vaccination with the nanovaccine resulted in higher levels of mucosal IgA and IgG than with an aqueous solution of soluble lipopolysaccharides and quillaja saponin. Systemic immunity triggered by the nanovaccine was evidenced by higher IgG levels in sera post priming and boosting. The nanovaccine induced a mixed Th1/Th2 type of immunity with higher IgG2a levels and thus a polarized Th1 response. The results suggest that the nanovaccine administered by homologous nasal route can prime the immune system via the mucosal and systemic pathways and is a good candidate for vaccine delivery.

1. Introduction

A recently emerging technology in the pharmaceutical industry employs supercritical fluids, which over their critical temperature demonstrate distinctive characteristics that aid nanoparticle formation (Padmajan Sasikala et al., 2016). Among the supercritical fluids, supercritical carbon dioxide—an odourless, colourless, highly pure, affordable, non-toxic, non-flammable, and recyclable gas with a very low critical point (critical temperature: 31.1 °C; pressure: 73 bar) is extensively used (Wang et al., 2016; Yen et al., 2011; Otero-Pareja et al., 2015; Hassan et al., 2004). Rapid expansion of supercritical solution (RESS) method involves the supersaturation and nucleation of a polymer when its supercritical solution is passed through an orifice under high pressure (Mullers et al., 2015). Polymeric nanoparticles prepared using this technology exhibit good flow properties and consistent particle size, which are critical for uniformity in subsequent pharmaceutical and biopharmaceutical processes.

Currently, vaccinations are the most widespread scheme of prophylaxis employed against brucellosis in countries with high occurance (Goodwin and Pascual, 2016). *B. abortus* strain 19 (S19) in cattle and *B. melitensis* strain Rev1 in sheep and goats in live attenuated or heat-killed forms are helpful vaccines (Kaynak-Onurdag et al., 2016; Li et al., 2015). Commercially available vaccines exhibit some detrimental traits, largely related to their partial avirulence and their abortifacient result when administered to pregnant animals (Moreno, 2014; Wang et al., 2014). A better prospect towards designing and preparing novel and efficient vaccines can involve inclusion of acellular components instead of the whole live or dead bacteria (Martins Rda et al., 2012). This strategy would overcome the main disadvantages of live attenuated vaccines and encourage the use of safer, more effective vaccines comprising acellular antigens (Pakzad et al., 2010). The prime-boost theory, conventionally derived from the same vaccine given few times over a definite period (homologous prime-boost), is currently applied also to the administration of the vaccine antigen in same (homologous prime-boost) or different (heterologous prime-boost) formulations (Wang and Wu, 2013; Radosevic et al., 2009; Lu, 2009; Rowland and McShane, 2011; Rowland et al., 2013; Mahomed et al., 2013).

Targeting mucosal sites by vaccination is essential considering that over 90% of infections occur at or through mucosal surfaces (Shakya et al., 2016). Local and systemic mucosal immunization has been shown to competently bring out humoral and cellular responses in animal models and humans (Lycke, 2012). The nasal route of immunization has

* Corresponding author at: Department of Pharmaceutical Sciences, Institute of Chemical Technology, Matunga, Mumbai 400019, India.
E-mail address: vb.patravale@ictmumbai.edu.in (V. Patravale).
[1] Authors have contributed equally to this work.

https://doi.org/10.1016/j.ijpx.2020.100053
Received 15 August 2019; Received in revised form 28 June 2020; Accepted 13 July 2020
Available online 30 July 2020

principally proved to be successful in activating memory immune responses both systemically and locally (respiratory, genital, and intestinal tracts) (Zuercher, 2003; Neutra and Kozlowski, 2006; Ciabattini et al., 2010). For devising a prime-boost vaccination approach, it is essential to portray the early events during the primary immune response, such as the increase in numbers of T-helper (Th) cell (CD4) upon antigen-MHC class II complex recognition. T-cell priming causes both B (immunoglobulins) and T-cell stimulation (Fiorino et al., 2013; Jiang et al., 2014). The antigen-specific CD4 T-cell primary activation following nasal immunization with soluble antigen mixed with mucosal adjuvants has been previously studied (Medaglini et al., 2006; Pettini et al., 2009).

The objective of this work was to develop a sub-unit vaccine (nanovaccine) for brucellosis that comprised sub-micron sized, mucoadhesive, biodegradable polymer-based particles using supercritical carbon dioxide for administration via the nasal mucosa in both animals and humans. The nanovaccine includes isolated lipopolysaccharides (LPS) from *Brucella spp*. (*B. abortus* strain S19) as antigenic components and quillaja saponin as an immunostimulant for induction of mucosal and systemic immunity against brucellosis. The innovativeness of the nanovaccine is orchestrated by the inclusion of xyloglucan, a tamarind seed derived polymer as a carrier with excellent mucoadhesive potential (Bhalekar et al., 2016). Xyloglucan can additionally facilitate continuous, prolonged antigen presentation to the underlying immunocompetent cells for inducing mucosal and systemic immunity. Saponin on the other hand, is a known immunoadjuvant for triggering humoral and cellular immunity (Cibulski et al., 2016a; Cibulski et al., 2016b). The nanovaccine employs LPS as antigens, which are non-whole cell components structurally specific to the *Brucella* spp. with known antigenicity. Anti-LPS antibodies have been identified in clinical samples of brucellosis infected patients (Sotnikov et al., 2015; Dorneles et al., 2015). LPS on their own are weakly immunogenic (Wong et al., 1992), and therefore, the work was aimed at delivering antigenic LPS with a combination of xyloglucan and saponins to induce a protective immune response with a prolonged release profile. The instigation of immune responses following intranasal priming and the secondary immune response after boosting by the homologous nasal route with the nanovaccine was studied in Balb/c mice. The *Brucella* antigen-specific IgA and IgG responses after nasal immunization were studied. The local and systemic antibody responses, as well as the IgG subtypes (IgG1 and IgG2a) following homologous prime-boost route were studied to determine if the immune response could trigger Th cell activity and if the Th response mechanism followed a dominant Th1 or Th2 type of activity.

2. Materials and methods

2.1. Subunit nanovaccine preparation using RESS

The RESS process was adopted to produce antigenic and immunogenic nanoparticles. The schematic procedure for the preparation of xyloglucan nanoparticles is illustrated in Fig. 1. The nanovaccine was designed using nanoparticles of xyloglucan (Glyloid 2A, Dainippon, Japan) manufactured using the environmentally non-hazardous RESS technology. The preparation of xyloglucan nanoparticles was achieved using supercritical carbon dioxide and is described briefly. Xyloglucan (2 g) was dissolved in deionized water (50 ml) at 70 °C with continuous stirring for 1 h, after which the solution was allowed to cool. Ethanol (50 ml) was added slowly to the solution and integrated within the aqueous xyloglucan solution with continuous overhead stirring to produce an ethanolic gel (2% *w/v*) of xyloglucan having 1:1 ethanol: water content. The ethanolic gel of xyloglucan was then fed into the RESS chamber and subjected to exposure of supercritical carbon dioxide (Critical point of carbon dioxide- 31.1 °C, 73.8 bar) with stirring for 10 min under pressure of 300 bar at 40 °C. This was followed by gradual release of supercritical carbon dioxide from the RESS chamber which also caused ejection of the nanoparticles from the exit portal and these nanoparticles were collected in a vessel in aqueous media (deionized water). The RESS instrument (Thar Instruments, Inc.) consisted of a reaction vessel (RESS chamber) and a nanoparticle collection vessel. The instrument also consisted of a CO_2 pump that was connected to a CO_2 cylinder, which introduced supercritical carbon dioxide into the RESS chamber via the inlet at a fixed flow rate (10 ml/min). The instrument operation was controlled by a computer software program (Thar Instruments, Inc.) which was used to adjust parameters such as pressure (bar) of CO_2 and temperature inside the RESS chamber. The RESS chamber also has an outlet (exit portal) connected to a valve operated nozzle through which the nanoparticles are released along with carbon dioxide and collected in the collection vessel. The collected nanoparticles were dried by vacuum drying and stored in vials.

The immunogenic nanoparticles were prepared as follows: Quillaja saponin (2 g) was dissolved in an aqueous solution of xyloglucan (cooled to room temperature, 30 °C) and this was further converted into an ethanolic gel (2% *w/v* xyloglucan, 1:1 water: ethanol). The gel was then fed into the RESS chamber and exposed to supercritical carbon dioxide at 40 °C, 300 bar pressure under stirring conditions for 10 min. The pressure in the chamber was then released gradually and immunogenic nanoparticles were collected at the outlet and vacuum dried. The nanoparticles were stored in sealed vials.

For preparing antigen loaded nanoparticles, xyloglucan nanoparticles were initially prepared by following method. Briefly, 2% w/v ethanolic gel of xyloglucan was subjected to the RESS process and the nanoparticles were subsequently collected and dried in a vacuum oven (37 °C, 24 h). For preparing LPS 50 μg per 25 μl dose, nanoparticles (4 mg/ml) were dispersed in 1 ml of phosphate buffer saline (PBS) (pH 7.4) in a vial. Then, a 1 ml of solution of LPS from *B. abortus* in PBS (4 mg/ml) was added to the nanoparticle dispersion (total volume 2 ml) and was incubated in a shaker incubator at 37 °C for 20 min. For preparing a dose of 10 μg LPS per 25 μl, a 1 ml solution of 0.8 mg/ml LPS was incubated with the nanoparticle dispersion. The particles were dried in a vacuum oven, stored in sealed vials. Subsequently, the subunit nanovaccine was prepared as follows: Immunogenic nanoparticles (1.5 mg/ml) were added to antigen loaded nanoparticles and dried in vacuum oven to obtain nanovaccine formulations having 100 μg fixed dose of quillaja saponin and varied doses (10 μg and 50 μg) of LPS per 25 μl. The formulations were re-dispersed in saline prior to use and evaluated.

2.2. Physicochemical evaluation

Particle morphology and size were determined by field emission scanning electron microscopy (FE-SEM) at Icon Analytical Equipment Pvt. Ltd., Mumbai, India. Dynamic light scattering (DLS) was further used to determine particle size of the nanovaccine using Zeta Sizer Nano ZS, Worcestershire, UK (Malvern Zetasizer 3000 HS and He/Ne laser at scattering angles of 173° at 25 °C). The Zeta Sizer Nano ZS instrument was also used to determine the surface charge by measuring zeta potential of the nanoparticles. Other physicochemical parameters such as viscosity (Ostwald viscometer), appearance and pH (Cyberscan pH meter, Eutech Instruments, Thermo Fisher Scientific, Inc.) were evaluated. The protocols for content determination of the antigen and immunoadjuvant are described in the supplementary material.

2.3. Content determination of antigen and immunoadjuvant

The content of LPS was determined by a previously reported method by (Warren et al., 1992). The thiobarbituric acid method was used to measure 2-keto, 3-deoxyoctulosonic acid (KDO), a cell wall component present in *B. abortus* LPS, for quantification of LPS in the nanovaccine. To conduct this assay, 100 μl of sodium periodate (meta) solution (0.2 M, in 9 M phosphoric acid) was added to 200 μl samples and incubated at about 30 °C for 20 min. Sodium arsenite (10%*w/v*, in a

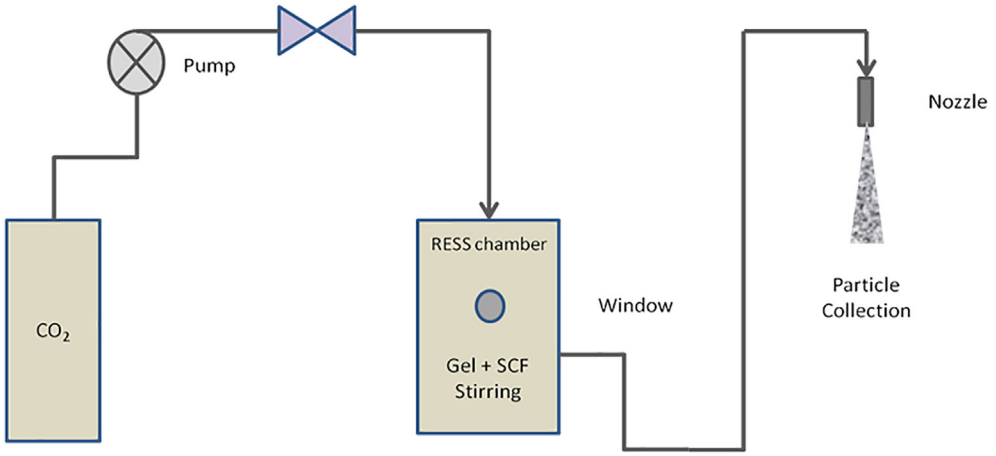

Fig. 1. Schematic representation of the RESS process for production of xyloglucan nanoparticles.

solution of 0.5 M sodium sulfate in 0.1 N H_2SO_4) was then added, shaken, and allowed to stand until the yellow-brown color disappeared. Thiobarbituric acid (0.6% *w/v*, in 0.5 M sodium sulfate) was then added and after shaking, the solution was heated in a vigorously boiling water bath for 15 min. The pink solution obtained was then allowed to cool to 4 ˚C for 5 min. At this juncture, the pink color of the solution faded and the solution became cloudy. This solution (1 ml) was added to an eppendorf containing cyclohexanone (1 ml) and shaken twice for KDO extraction. The contents were then centrifuged (10,000 × g, 3 min) and the optical density (OD) of the organic layer was measured using a spectrophotometer (Multiskan Go™, Thermo Fisher Scientific Inc., USA) at 549 nm. Millipore water (200 µl) was used as blank, the nanovaccine (without LPS) was used as control and LPS from *B. abortus* was used as standard.

The content of quillaja saponin in the nanovaccine was determined using orcinol sulfuric acid method (Behboudi et al., 1995). To 1 ml of sample, 2 ml of orcinol reagent (0.3% w/v of 3,5-dihydroxytoluene monohydrate in concentrated sulfuric acid) was added, mixed and incubated for 15 min at room temperature (30 ˚C). The sample was boiled for 20 min and then cooled on ice to room temperature. After 10 min, OD readings were recorded at 520 nm using a spectrophotometer (Multiskan Go™, Thermo Fisher Scientific Inc., USA). Millipore water (1 ml) was used as blank, nanovaccine (without quillaja saponin) as control and Quillaja saponin (Sigma Aldrich, USA) as standard. The release profile was calculated in terms of percentage cumulative release and plotted against time.

2.4. Stability studies

Stability studies were conducted as per ICH guidelines – Q5C for biotechnological products. The nanovaccine formulation was subjected to accelerated stability testing at 40 ˚C ± 2 ˚C, 75% RH ± 5% RH for climatic zone III. The nanovaccine formulation was also assessed for long term stability for 1 year by periodically measuring particle size and content at 0, 3, 6 and 12 months at 30 ˚C ± 2 ˚C, 65% RH ± 5% RH for climatic zone III. The content of LPS and quillaja saponin in the nanovaccine was determined by performing thiobarbituric and colorimetric assays, respectively (described above).

2.5. Endotoxin content determination

The endotoxin content in the nanovaccine was determined using Pierce LAL (*limulus amebocyte lysate*) chromogenic endotoxin quantitation kit purchased from Thermo Scientific Inc., USA. Serial dilutions of the nanovaccine were prepared and the OD value that fit within the range of the standard curve (as per Beer Lambert's law) was recorded and the endotoxin content was subsequently calculated. The protocol for determination of endotoxin content per kit manufacturer's instructions is the following. Briefly, the microplate was equilibrated in a heating block for 10 min at 37 ˚C. With the microplate maintained at 37 ˚C, 50 µl of each standard or unknown sample replicate was carefully dispensed into the appropriate microplate well which was then covered with the lid and incubated for 5 min at 37 ˚C. Subsequently, 50 µl of LAL was added to each well using a pipettor, the plate covered with the lid and gently shaken for 10 s. The plate was incubated at 37 ˚C for 10 min. After exactly 10 min, 100 µl of substrate solution was added to each well. The substrate solution was then pipetted in the wells by maintaining a consistent pipetting speed. The plate was then covered with the lid and gently shaken for 10 s. The plate was incubated again at 37 ˚C for 6 min. Following this, 50 µl of Stop Reagent (25% v/v acetic acid) was added to the wells and the plate was gently shaken for 10 s. The absorbance was measured at 405 nm on a plate reader. The average absorbance of the blank (pyrogen-free water supplied with the kit) replicates was subtracted from the average absorbance of all individual standard and unknown sample replicates. A standard curve was prepared by plotting the average blank-corrected absorbance for each standard versus its concentration in EU/ml.

2.6. In vitro release studies

The in vitro release studies were performed on the nanovaccine to determine the release characteristics of the loaded antigen and immunoadjuvant. The nanovaccine was analyzed in vitro to study the release profile of the antigen. The nanovaccine (100 mg) loaded with LPS (antigen) was dispersed in 5 ml of phosphate buffer saline (pH 6.8, 0.01% sodium azide). The release study was conducted under horizontal agitation for 12 days. Aliquots of 1 ml were withdrawn at intervals of 2 h, 4 h, 8 h, 12 h, 24 h, 2 d (day), 3 d, 4 d, 8 d, 10 d and 12 d, and replaced by fresh medium. Xyloglucan nanoparticles (without LPS) were used as control and subjected to the same procedure. The aliquots were centrifuged (20,000 × g, 10 min) and assessed for LPS content in the supernatant using thiobarbituric assay for LPS determination (Supplementary material). The nanovaccine was also characterized for determining the in vitro release profile of the immunoadjuvant. The nanovaccine (100 mg) comprising quillaja saponin (immunoadjuvant) was dispersed in 5 ml of phosphate buffer saline, pH 6.8. The release study was conducted under horizontal agitation for 12 d. Aliquots of 1 ml were withdrawn at intervals of 2 h, 4 h, 8 h, 12 h, 24 h, 2 d, 3 d, 4 d, 8 d, 10 d and 12 d, and replaced by fresh medium. Xyloglucan nanoparticles (without quillaja saponin) was used as control and subjected to the same procedure. The aliquots were centrifuged (20,000 x g, 10 min) and assessed for quillaja saponin content in the

supernatant using colorimetric assay for quillaja saponin content determination (Supplementary material). Experiments were run in triplicate for each time point of the release study. The results are expressed in terms of percentage cumulative release and plotted against time.

2.7. Ex vivo assessment of nanovaccine interactions with nasal mucosa

Mucoadhesion of the nanovaccine formulation was assessed using texture analyzer (TA-XT Plus) equipped with a 5 kg load cell and 10 mm plastic cylindrical probe. The mucoadhesion potential of the nanovaccine was tested using goat nasal mucosa. Approximately 0.2 ml of nanovaccine formulation was uniformly spread over the probe which was then brought into contact with the goat mucosa and held for 60 s. The force of detachment of the probe from the goat mucosa was measured at a pre-test speed of 2 mm/s, test speed of 1 mm/s, post-test speed of 10 mm/s and acquisition rate of 100 points/s. Trigger type was set to auto-0.01 g while tare mode was set to auto with the option of return to start. The mucoadhesion potential of the nanovaccine formulation was compared against vehicle control (phosphate buffer saline, pH 6.8) and plain xyloglucan (Glyloid 2A). The values of the peak force (N) and work of adhesion (N.*sec*) were recorded and compared. The mucoretentive ability of the nanovaccine formulation on goat nasal mucosa was also assessed. The study was performed by applying Rhodamine B loaded nanovaccine to goat nasal mucosa using the method reported by Mumtaz with little modification (Mumtaz and Ching, 1995). A strip of goat nasal mucosa was mounted on a glass slide and nanovaccine (100 µl) was applied to the mucosal surface. This glass slide was incubated for 15 min to allow the nanovaccine to interact with the membrane and finally placed in the cell that was attached to the outer assembly at an angle of 45°. Phosphate buffer saline (pH 6.8, with 0.1% sodium azide) was circulated to the cell over the nanovaccine and membrane at the rate of 1 ml/min with the help of pump. The images of the mucosa were taken at time 30 min, 1 h, 2 h, 4 h, 8 h, 12 h, 24 h and 2 d.

2.8. In vivo nasal ciliotoxicity evaluation

Nasal ciliotoxicity evaluation of the nanovaccine was conducted in female rats (Protocol No.: CPCSEA-BCP/2015-01/02). For this study, nanovaccine loaded with higher dose of antigen (NV 50) was tested. In this evaluation, fifteen female Sprague Dawley rats (6 to 8 weeks age) were randomized into various groups (three animals per group), vehicle control, negative control, blank formulation (without the antigen and immunoadjuvant), nanovaccine (NV 50)-first dose and nanovaccine (NV 50)-booster dose. All the treatments were administered in the final volume of 25 µl, using a pipette into the nostrils of the animals. Single (first) dose groups (administered on day 1) were sacrificed on day 3 and booster dose groups (administered on day 14) were sacrificed on day 17 of the experimental period. The nasal mucosa was dissected and stored in 10% buffered formalin solution until histopathological evaluation. The tissue samples were stained using Hematoxyline-Eosin and examined microscopically for cellular damage and intactness of the nasal cilia. Sodium deoxycholate (0.1%) and saline were employed as negative and vehicle controls respectively.

2.9. Immunization studies in Balb/c mice

Fifty female Balb/c mice (8 weeks old) were housed under standardized laboratory conditions at a temperature of 25 ± 1 °C and exposed to a regular light/dark schedule. They were maintained under pathogen free conditions and, food and water were provided ad libitum. All animals were fed a standard rat chow. All animal experiments were approved by the Institutional Animal Ethics Committee (Protocol No.: CPCSEA-BCP/2015–01/01). The mice were randomized in five groups (n = 6 per group) and were immunized on day 1 (initial dose) and day 14 (week 2, prime booster dose) intranasally. All the treatments were administered in the final volume of 25 µl. Blood samples were taken from the temporal plexus every 7th day after the initial dose administration under anesthesia and the sera collected were stored at −20 °C. On day 42 (week 6), all of the mice were sacrificed post blood collection and subsequently, bronchoalveolar fluid (BALF) samples were collected. The sera and BALF samples were analyzed for antibody secretion using enzyme-linked immunosorbent assay (ELISA). The commercial ELISA kits (My Biosource, USA) were employed to determine *Brucella* antibodies from BALF (IgA and IgG) and in sera (IgG, IgG1 and IgG2a).

2.9.1. IgA determination

BALF samples were analyzed undiluted to determine IgA levels by indirect ELISA method. The protocol was supplied by the manufacturer and is as follows. Briefly, 100 µl of samples were pipetted into predesignated wells of the micro titer plates. 100 µl of PBS (pH 7.0) was added to each of the blank control wells. The micro titer plates were covered and incubated at room temperature (30 ± 2 °C) for 60 ± 2 min. Following incubation, the contents of the wells were aspirated and the plates washed using washing buffer four times. Then, 100 µl of Enzyme-Antibody Conjugate was pipetted to each well, and the micro titer plates were covered and incubated in the dark at 25 °C for 30 ± 2 min. The contents of the plates were aspirated and washed again four times. Subsequently, 100 µl of 3,3′,5,5′-Tetramethylbenzidine (TMB) Substrate Solution was added into each well and the plates were incubated in the dark at 25 °C for precisely 10 min. After 10 min, 100 µl of Stop Solution was added to each well and OD values were recorded at 450 nm using ELISA plate reader (MultiskanGo, Thermo Scientific Inc., USA). By using the results observed for the standards, a second order polynomial (quadratic) standard curve was constructed. The test sample values were interpolated from standard curve and corrected for sera dilution factor to arrive at the IgA concentration (ng/ml) in original samples.

2.9.2. IgG determination

Serum samples diluted 1/40000 in the dilution buffer provided by the manufacturers and BALF samples (undiluted) were analyzed for IgG levels using the competitive ELISA method. The protocol was supplied by the manufacturer and is as follows. Briefly, 100 µl of samples were pipetted into pre designated wells of the micro titer plates. 100 µl of PBS (pH 7) was added to the blank control wells. 50 µl of Enzyme-Conjugate was added to each well (except blank) and mixed. The micro titer plates were covered and incubated at 37 °C for 60 ± 2 min. Following incubation, the contents of the wells were aspirated and the plates were washed using washing buffer for five times. Then, 50 µl of TMB Substrate Solution was pipetted to each well, and the micro titer plates were covered and incubated in the dark at 37 °C for 10–15 min. After this, 50 µl of Stop Solution was added to each well and optical density values were recorded immediately at 450 nm using ELISA plate reader (MultiskanGo, Thermo Scientific Inc., USA). By using the results observed for the standards, a second order polynomial (quadratic) standard curve was constructed. The test sample values were interpolated from standard curve and corrected for sera dilution factor to arrive at the IgG concentration (ng/ml) in original samples.

2.9.3. IgG1 determination

Serum samples diluted 1/40000 in the dilution buffer provided by the manufacturers were analyzed for IgG1 levels using the indirect ELISA method. The protocol was supplied by the manufacturer and is as follows. Briefly, 100 µl of samples were pipetted into pre-designated wells of the micro titer plates. The micro titer plates were covered and incubated at 25 °C for 60 ± 2 min. Following incubation, the contents of the wells were aspirated and the plates washed using washing buffer four times. Then, 100 µl of Enzyme-Antibody Conjugate was pipetted to each well, and the micro titer plates were covered and incubated in the dark at 25 °C for 20 ± 2 min. The contents of the plates were aspirated and washed again four times. Subsequently, 100 µl of TMB Substrate

Solution was added into each well and the plates were incubated in the dark at room temperature for precisely 10 min. After 10 min, 100 µl of Stop Solution was added to each well and OD values were recorded at 450 nm using ELISA plate reader (MultiskanGo, Thermo Scientific Inc., USA). By using the results observed for the standards, a second order polynomial (quadratic) standard curve was constructed. The test sample values were interpolated from standard curve and corrected for sera dilution factor to arrive at the IgG1 concentration (ng/ml) in original samples.

2.9.4. IgG2a determination

Serum samples diluted 1/40000 in the dilution buffer provided by the manufacturers were analyzed for IgG2a levels using the indirect ELISA method. The protocol was supplied by the manufacturer and is as follows. Briefly, 100 µl of samples were pipetted into pre designated wells of the micro titer plates. The micro titer plates were covered and incubated at 25 °C for 60 ± 2 min. Following incubation, the contents of the wells were aspirated and the plates washed using washing buffer four times. Then, 100 µl of Enzyme-Antibody Conjugate was pipetted to each well, and the micro titer plates were covered and incubated in the dark at 25 °C for 20 ± 2 min. The contents of the plates were aspirated and washed again four times. Subsequently, 100 µl of TMB Substrate Solution was added into each well and the plates were incubated in the dark at room temperature for precisely 10 min. After 10 min, 100 µl of Stop Solution was added to each well and optical density values were recorded at 450 nm using ELISA plate reader (MultiskanGo, Thermo Scientific Inc., USA). By using the results observed for the standards a second order polynomial (quadratic) standard curve was constructed. The test sample values were interpolated from standard curve and corrected for sera dilution factor to arrive at the IgG2a concentration in original samples.

2.10. Statistical analysis

Values for in vitro release, stability studies, and mucoadhesion analyses are expressed as mean ± SD ($n = 3$). One-way ANOVA with Bonferroni correction was applied to the data from mucoadhesion studies to test significance of the results ($P < .05$). For ELISA results, the values representing antibody levels are expressed as mean ± SEM. Statistical analyses were performed using GraphPad Prism Version 5.0 software. The differences between the groups were analyzed with one-way ANOVA, followed by post hoc analysis with Bonferroni's test for BALF IgA and IgG determinations. For serum IgG, IgG1 and IgG2a measurements, two-way ANOVA (with time and treatment as variables), followed by Bonferroni's test was used. Statistical significance was considered at $P < .05$.

3. Results

3.1. Preparation of subunit nanovaccine

Xyloglucan (Glyloid 2A) composed of polysaccharides, is insoluble in non-polar CO_2. Therefore, a new technology was developed in which homogenous ethanolic gels of xyloglucan were prepared and the inclusion of ethanol led to the formation of nanoparticles. The nanoparticle production was a result of the supersaturation of xyloglucan in the gel triggered by the rapid solubilization of ethanol from the gel in supercritical CO_2 (which acted as a non-solvent) in the RESS chamber.

The nanoparticle production was optimized using the classical method of optimization – by studying formulation and process related factors that could control the particle size during production. Pressure and temperature within the RESS chamber were identified as process related factors and ethanol content in the xyloglucan ethanolic gel was categorized as the formulation related factor. To study the effect of ethanol content on particle size of xyloglucan nanoparticles, the amount of ethanol in the 2% (*w/v*) homogenous ethanolic gel of xyloglucan was varied. The pressure (300 bar) and temperature (40 °C) inside the RESS chamber were kept constant. For a 2% w/v xyloglucan gel, at least 30% *v*/v ethanol content is required to form gel and the viscosity of the gel increases with higher ethanol content. However, 30% v/v ethanol content produced particles in the micro range. As shown in Fig. S1, gels with an ethanolic content of 50% v/v or greater produced nanosized xyloglucan particles. With respect to the xyloglucan content, gels having more than 2.5% w/v of xyloglucan resulted in formation of large fibres and microparticles. By contrast, gels with xyloglucan content < 1.5% w/v did not elicit nanoparticle formation irrespective of the ethanol content.

For studying the effect of pressure on the size of xyloglucan particles, the temperature and ethanol content were kept constant at 40 °C and 50% *v*/v, respectively. As shown in Fig. S2, increase in pressure within the RESS chamber beyond 200 bar produced nanoparticles. Further, upon studying the effect of varying temperatures on the particle size, it was found to be inversely proportional (Fig. S3).

The desired range of nanoparticle size was 250–350 nm, as then, these particles can easily get entrapped within the 'net' of the nasal mucosal lining slowly releasing the antigen and immunoadjuvant in the nasal mucosa associated lymphoid tissue (MALT), and through the sinus drain, into the lymph nodes for exposure to circulating antigen presenting cells (APCs) for generation of systemic immunity along with mucosal immune responses (Bernocchi et al., 2017). Nanoparticles of size 300 nm were obtained at 40 °C at pressure of 300 bar (with xyloglucan gels having 50% v/v ethanolic content). The RESS procedure was thus optimized to generate nanoparticles of the desired size range (250–350 nm) at temperatures as low as 40 °C.

3.2. Physicochemical evaluation

The pH of the nanovaccine formulation was found to be 6.58. The nanovaccine formulations appeared translucent upon reconstitution with purified water and the viscosity of the reconstituted nanovaccine was found to be 23 cps. The surface charges of nanoparticles were close to neutral with slight negative potential (−1.66 mV) measured at 25 °C. The nanovaccine showed irregularly shaped nanoparticles in the range of 250–350 nm (Fig. 2A) and concurred with the data obtained from dynamic light scattering (297.3 nm) (Fig. 2B). Irregularly shaped particles are easily captured by the immune cells of the reticuloendothelial system and are therefore beneficial as efficient vaccine delivery carriers (Moon et al., 2012).

3.3. Content determination of antigen and immunoadjuvant

The 2-keto, 3-deoxyoctulosonic acid (KDO) sugar is an inherent component of LPS of the *B. abortus* strain. The thiobarbituric acid assay involves extraction of this KDO sugar from LPS, which can be measured colorimetrically and employed to back calculate the amount of LPS. The content of LPS in the nanovaccine loaded with 50 µg LPS was calculated to be 54.08 ± 0.36 µg/ml using the standard curve shown in Fig. S4. Similarly, in the nanovaccine loaded with 50 µg LPS, it was 11.38 ± 0.8236 µg/ml. Similarly, quillaja saponin content was determined using colorimetric orcinol sulfuric acid assay method and the content in the nanovaccine was found to be 105.05 ± 0.51 µg/ml, calculated using the standard curve shown in Fig. S5.

3.4. In vitro release study

Phosphate buffer saline pH 6.8 was used as the release medium as nasal fluid has a pH of 6.0 to 7.0. Fig. 3 shows the release profile of LPS from the nanovaccine. The release profile exhibited by the antigen is a two-stage sustained release profile, characterized by an initial release of 26% within the first 24 h followed by a more continuous and progressive release of the loaded antigen. The LPS gradually release from the nanoparticles for up to 12 d (85%), exhibiting a sustained release

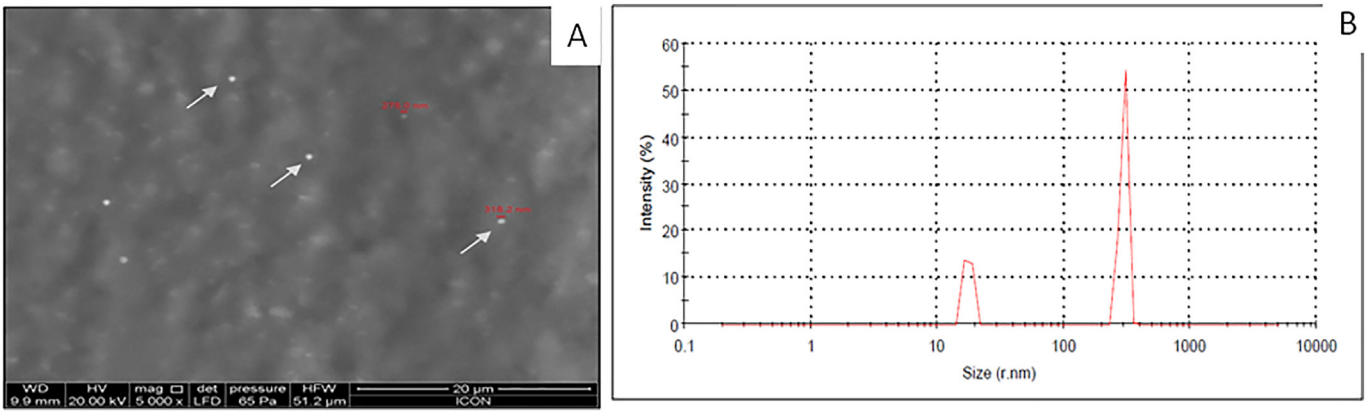

Fig. 2. (A) FE-SEM image, and (B) dynamic light scattering data of the nanovaccine.

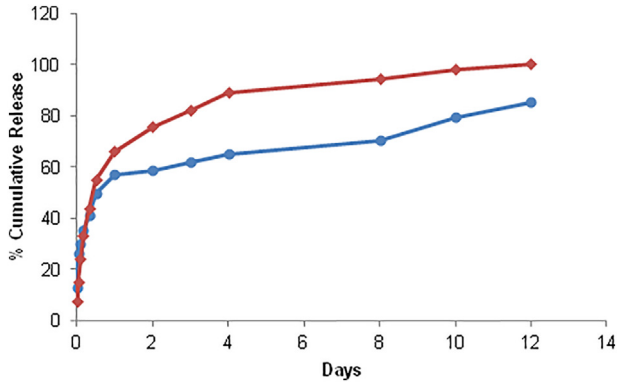

Fig. 3. In vitro cumulative release of lipopolysaccharides (antigen) (blue) and quillaja saponin (immunoadjuvant) (red) from nanovaccine. Values are expressed as mean ± SD. (For interpretation of the references to color in this figure legend, the reader is referred to the web version of this article.)

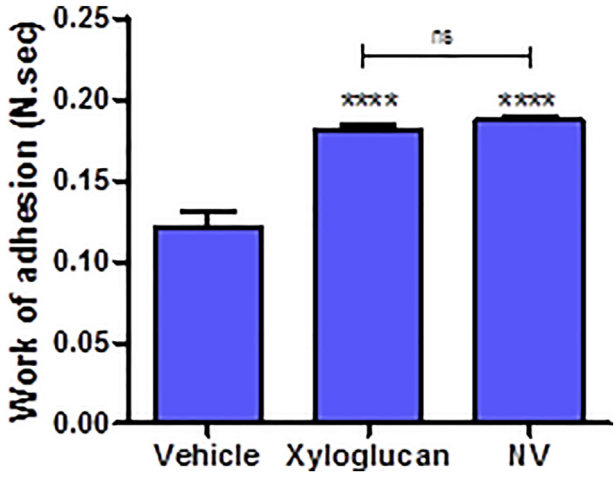

Fig. 4. Mucoadhesion exhibited by the nanovaccine (NV) in comparison to xyloglucan. Values are expressed as mean ± SD. One way ANOVA with Bonferroni correction was applied to test significance of the results (****P < .0001, ns – not significant).

pattern (Fig. 3). This is significant since the nanoparticles can sustain antigen release up to the time for administration of the booster dose.

Fig. 3 also depicts the release profile of quillaja saponin from the nanovaccine in which a sustained release pattern, characterized by an initial release of about 15% within the first 12 h and later, a persistent and sustained release pattern of the loaded antigen was observed. The immunoadjuvant too was gradually released from the nanoparticles for up to 12 d. The in vitro release results confirm the potential of the nanovaccine to function as a depot at the mucosal site for gradual release of the antigen and the immunoadjuvant. Further, the simultaneous steady release of the components can stimulate the induction of the secondary immune response to produce protective antibodies against *Brucella*.

3.5. Nasal mucoadhesion and mucoretention time

Mucoadhesion studies were conducted to assess the mucoadhesive capabilities of the formulation to the nasal mucosa, the site where the nanovaccine would be administered to ensure exposure to the MALT for a prolonged period to activate mucosal and systemic immunity. Mucoadhesion studies showed that the nanovaccine had strong nasal mucoadhesive properties. The work of adhesion of the nanovaccine formulation was nearly same as that of xyloglucan alone (Fig. 4). The results thus implied that the mucoadhesion capacity of the nanovaccine was as strong as that of the original polymer.

The nanovaccine formulation was retained for more than 24 h on goat mucosal tissue (Fig. S6). Sodium azide was included in the buffer media to prevent tissue deterioration during the study. Xyloglucan interacts with the mucosal lining by virtue of strong hydrogen bonding due to abundance of hydroxyl groups in its structure (Barbi Mda et al., 2015). This mucoadhesive property of xyloglucan is well reflected in the nanovaccine formulation, affording strong mucus binding capabilities to the nanovaccine.

3.6. Stability studies and bacterial endotoxin content

The particle sizes and content do not show significant changes over 12 months when subjected to long term stability testing (Table 1). Therefore, the nanovaccine is very stable and has a shelf life of at least one year at room temperature conditions for Climatic Zone III as per ICH. The nanovaccine is packaged in dry powder form, which renders prolonged stability on shelf.

For determining bacterial endotoxin content of the nanovaccine, a standard curve (Fig. S7) was constructed using the standard endotoxin. The bacterial endotoxin content of the nanovaccine was found to be 11 EU/ml, which is within acceptable limits (< 200 EU/ml) for vaccines (Mathaes et al., 2014).

3.7. In vivo nasal ciliotoxicity evaluation

A total evaluation of nasal toxicity must reflect on damage to nasal epithelial cells, and effects on nasal ciliary function (motility). The nanovaccine was assessed for nasal ciliotoxicity in Sprague Dawley rats. Tissue samples were collected and subjected to histopathological analysis. The nanovaccine showed no obvious indications of ciliary

Table 1
Long term stability data according to ICH Q5C guidelines for biotechnological products. Content values are expressed as mean ± SD.

	Property	0 months	3 months	6 months	12 months
1.	Particle Size	297.3 nm	296.5 nm	296.1 nm	293.6 nm
2.	Quillaja Saponin content	103.49 ± 0.26 µg	97.22 ± 0.52 µg	101.53 ± 0.87 µg	95.45 ± 0.25 µg
3.	LPS content	57.03 ± 1.52 µg	58.67 ± 1.14 µg	52.87 ± 2.05 µg	56.33 ± 4.06 µg

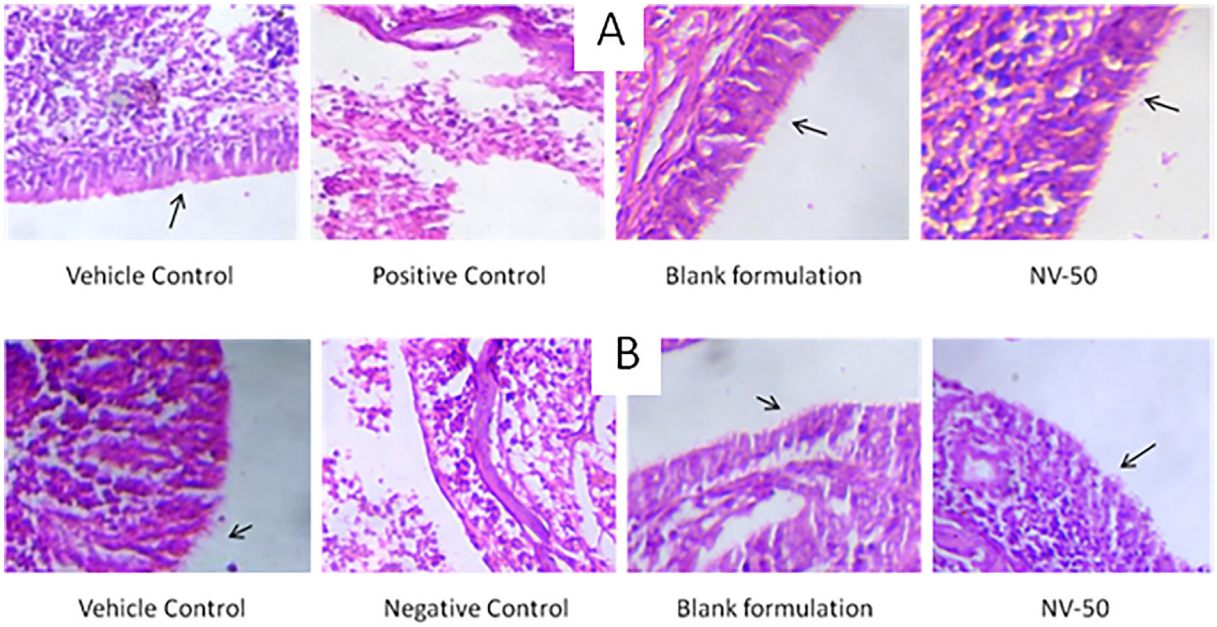

Fig. 5. Images of rat nasal tissues obtained by histopathological evaluation for (A) Single dose administration, day 1, and (B) Booster dose administration, day 14 for treatment groups of vehicle control, positive control, blank formulation and nanovaccine (NV 50).

toxicity. In the saline group (vehicle control), the cilia were arranged in neat rows and distributed on the surface of the rat nasal mucosa. Akin to the vehicle control group, the nanovaccine treated group both at first dose (day 1) (Fig. 5A) and booster dose (day 14) (Fig. 5B) administration did not show any ciliary damage or loss, lodging or other anomalies and epithelial cells damage. In comparison, sodium deoxycholate (negative control) showed significant damage to the mucosa and epithelia eliciting high ciliary toxicity.

3.8. Evaluation of immune responses

The immunogenic activity of the developed nanovaccine formulations administered intranasally in female Balb/c mice was evaluated by measuring IgA and IgG levels in the nasal washes (BALF). Fig. S8 depicts the polynomial standard curves that were constructed for determining IgA and IgG levels from BALF using the indirect ELISA method. A significantly higher production of IgA was seen in mice primed and boosted by the nanovaccine compared to the control group (Fig. 6A). In comparison to the groups which were administered only antigen-immunoadjuvant solutions (LPS 10 and LPS 50), the nanovaccine groups NV 10 and NV 50 exhibited higher IgA responses. The IgA levels were however not found to be dependent on the dose of the antigen (LPS), as both the nanovaccine groups showed nearly equivalent IgA levels which was in concurrence with similar observation seen with groups that were administered antigen solutions. Similarly, the nanovaccine formulations also showed (Fig. 6B) significantly higher *Brucella* specific IgG antibodies in the BALF of Balb/c mice compared to control (saline treated) mice four weeks after booster dose administration. The IgG levels of the nanovaccine administered groups were higher than the levels shown by antigen-immunoadjuvant solutions. Interestingly, both the IgG and IgA levels of NV 10 were higher than LPS 50, implying that the nanovaccine components together considerably boosted the mucosal immunity induced by the antigen.

Further development of systemic immunity in Balb/c mice prime boosted at week 2 via the homologous intranasal route was determined by periodically assessing serum samples every week. Fig. S8B shows polynomial standard curve used to determine IgG levels. It was found that IgG antibodies were significantly higher in mice immunized with the nanovaccine than control mice (Fig. 7). Boosting caused a rapid increase in IgG levels of mice vaccinated by both NV 10 and NV 50, with NV 50 showing a higher and more sustained response than NV 10. In the NV 50 vaccinated group, the IgG levels persisted up to 4 weeks post prime boosting. Although NV 10 too exhibited a significant systemic immune response after prime boosting, NV 50 showed a relatively prolonged systemic immune response than NV 10 (which lasted up to 2 weeks post boosting). The nanovaccine groups demonstrated better systemic IgG responses than the mice immunized with antigen-immunoadjuvant solutions. LPS 50 exhibited a comparatively higher immune response 1 week post boosting than LPS 10, but in the later weeks the IgG levels reduced and followed a pattern similar to that of LPS 10. Fig. S9 shows week wise intergroup comparative results seen in Balb/c mice.

The development of T-cell mediated immunity was assessed by determining levels of IgG2a (Th1 type) and IgG1 (Th2 type). To study the type of Th response, the distribution of IgG subclasses was assessed in the sera of all animals. Fig. S10 depicts the standard curves used to determine IgG1 and IgG2a levels using indirect ELISA. Mice primed by the intranasal route with the nanovaccine formulations produced higher levels of *Brucella* specific IgG2a antibodies compared to mice administered with antigen-immunoadjuvant solutions, one week post boosting (Fig. 8). Similar observations were seen in *Brucella* specific IgG1 levels. Significant levels of IgG2a and IgG1 demonstrated a mixed

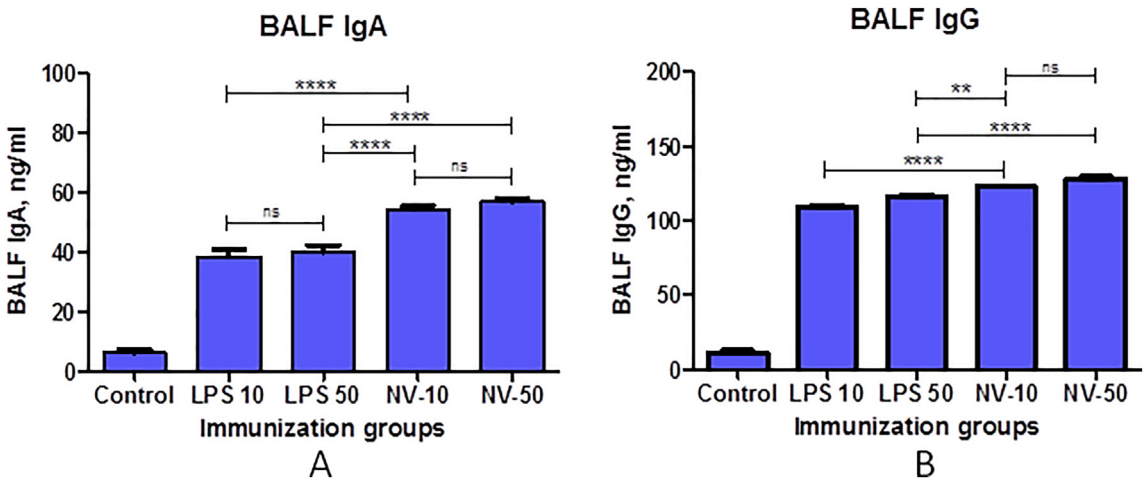

Fig. 6. Balb/c mice were immunized with nanovaccine loaded with LPS and quillaja saponin (immunoadjuvant) at day 0, boosted at day 14 (week 2) by the intranasal route. The antibody responses in bronchoalveolar lavage fluid (BALF) were assessed by ELISA. (A) *Brucella* specific IgA responses assessed in samples collected on day 42 (week 6), and (B) *Brucella* specific IgG responses assessed in samples collected on day 42 (week 6). Values are expressed as mean ± SEM ($n = 6$ for all groups). Statistical analysis was performed by using one-way analysis of variance (ANOVA), followed by Bonferroni's test as a post hoc analysis to identify significant differences among the groups. *LPS 10 – LPS 10 μg and immunoadjuvant 100 μg; LPS 50 – LPS 50 μg and immunoadjuvant 100 μg; NV 10 – Nanovaccine with LPS 10 μg and immunoadjuvant 100 μg; NV 50 – Nanovaccine with LPS 50 μg and immunoadjuvant 100 μg. *P* values: $*P < .05$, $**P < .01$, $***P < .001$, $****P < .0001$.

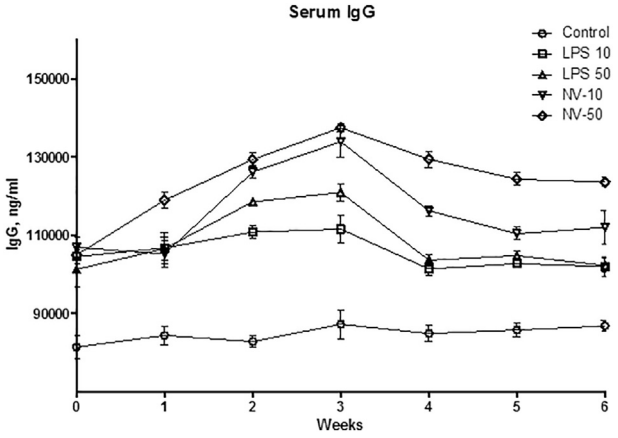

Fig. 7. IgG antibody responses in sera at weeks 0, 1, 2, 3, 4, 5, and 6. Values are as mean ± SEM (n = 6 for all groups). *LPS 10 – LPS 10 μg and immunoadjuvant 100 μg; LPS 50 – LPS 50 μg and immunoadjuvant 100 μg; NV 10 – Nanovaccine with LPS 10 μg and immunoadjuvant 100 μg; NV 50 – Nanovaccine with LPS 50 μg and immunoadjuvant 100 μg.

type of immune response, confirming activation of both Th1 and Th2 type of responses. Further, mixed Th1/Th2 responses persisted throughout 6 weeks of the study. The IgG2a/IgG1 ratios (> 1 for nanovaccine and antigen-immunoadjuvant solution treated groups) calculated for sera collected every week (Fig. 9) revealed a Th1 dominant response throughout. The prevailing mechanism of immune response suggested by the data agrees with the investigations that propose the manifestation of Th1 dominant protective immune responses elicited by most *Brucella* vaccines (Avachat et al., 2013; Brito and Singh, 2011). Thus, the results suggest a mixed immune response with a stronger Th1 polarization in mucosally primed mice.

4. Discussion

Vital parameters of prolonged vaccine efficacy are the persistence of antibodies, reliant upon prolonged antigen exposure to APCs such as microfold or M cells and dendritic cells, and the concomitant generation of immune memory cells. T-cells are essential to the stimulation of pathogen specific antibodies and immune memory, thus becoming key initiators of the holistic immune response from the time of primary immunization. In this work, the primary expansion of antigen-specific immunoglobulins following homologous intranasal immunization has been explored in Balb/c mice. Specifically, the levels of IgA and IgG have been studied in nasal mucosal tissues, as indicators of induction of mucosal immunity and levels of IgG, IgG1, and IgG2a in sera to deduce the stimulation and endogenous mechanism of the systemic immune response. Intranasally delivered soluble antigens were gradually released from the nanovaccine formulation and exposed to the APCs within MALT and later circulating dendritic cells in lymph nodes. Saponins from *Quillaja saponaria* bark extract used as the immunoadjuvant in the nanovaccine formulation are surface-active agents binding to hydrophobic surfaces of immune cells and elicit their immunostimulatory properties. Quillaja saponins co-released with the antigen from the nanovaccine mediated the antigenic recognition by the APCs inducing an effective and quicker onset of APC-triggered major histocompatibility complex (MHC) Class II mediated immune activation. This triggered active secretion of protective IgA and IgG antibodies in the nasal mucosa as a manifestation of the primary defense mechanism was detected at the end of 6 weeks, thus confirming prolonged mucosal immunity.

The mucosal immune response observed in Balb/c mice vaccinated intranasally with nanovaccine formulations is higher than the one observed in Balb/c mice following nasal immunization with antigen-immunoadjuvant solutions. Antigen solutions alone induce considerably low immunogenic responses (Wong et al., 1992), and therefore the potency of the nanovaccine was compared against antigen-immunoadjuvant solutions; interestingly the nanovaccine formulations showed an immune response that was at least 1.5 fold higher. The nanovaccine formulations aided gradual exposure of the antigen and immunoadjuvant to the APCs in MALT ensuring clonal expansion of secretory immunoglobulins. The nanovaccine reasonably demonstrated potential to instigate mucosal immunity for at least 6 weeks post immunization.

Nasal immunization further conferred the manifestation of systemic immunity by eliciting considerably higher levels of serum IgG antibodies, which persisted for at least 6 weeks after priming. Booster vaccination with both the nanovaccine formulations induced a considerable and swift rise of the serum IgG antibody levels. Nanovaccine

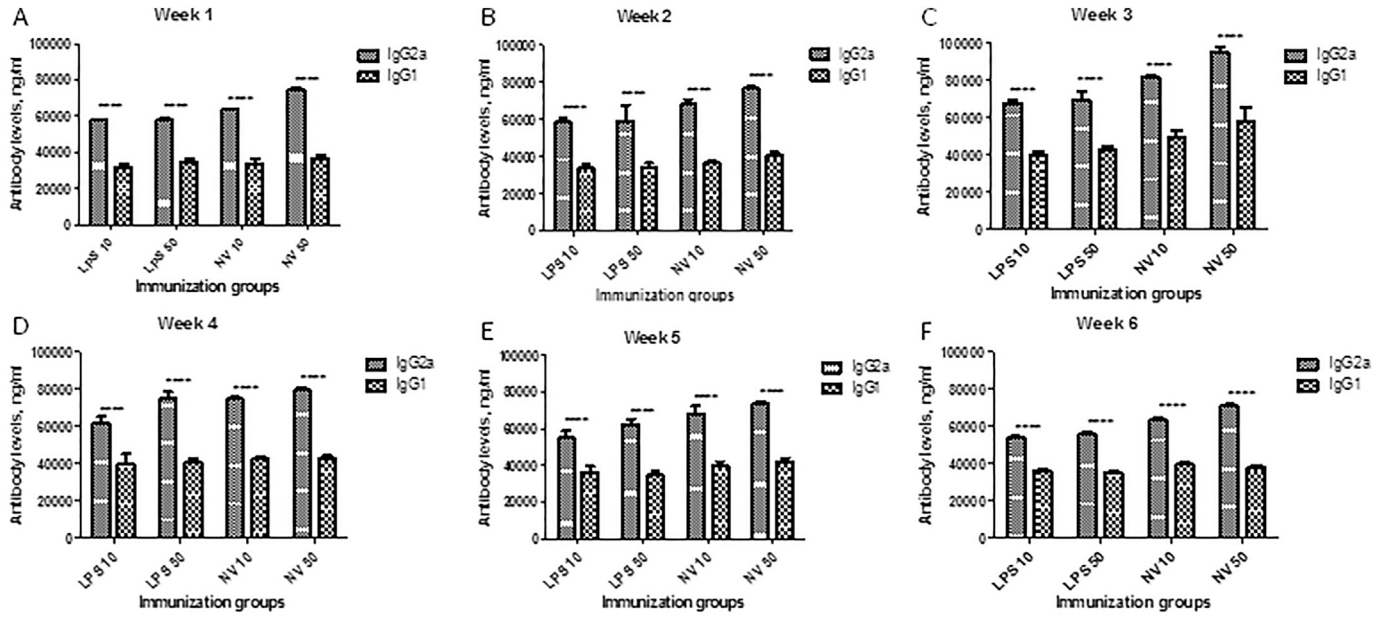

Fig. 8. Relative comparison between IgG2a and IgG1 levels in sera at weeks (A) 1, (B) 2, (C) 3, (D) 4, (E) 5, and (F) 6, respectively. LPS 10 – LPS 10 μg and immunoadjuvant 100 μg; LPS 50 - LPS 50 μg and immunoadjuvant 100 μg; NV 10 – Nanovaccine with LPS 10 μg and immunoadjuvant 100 μg; NV 50 – Nanovaccine with LPS 50 μg and immunoadjuvant 100 μg. Values are expressed as mean ± SEM. *P* values: $^{*}P < .05$, $^{**}P < .01$, $^{***}P < .001$, $^{****}P < .0001$.

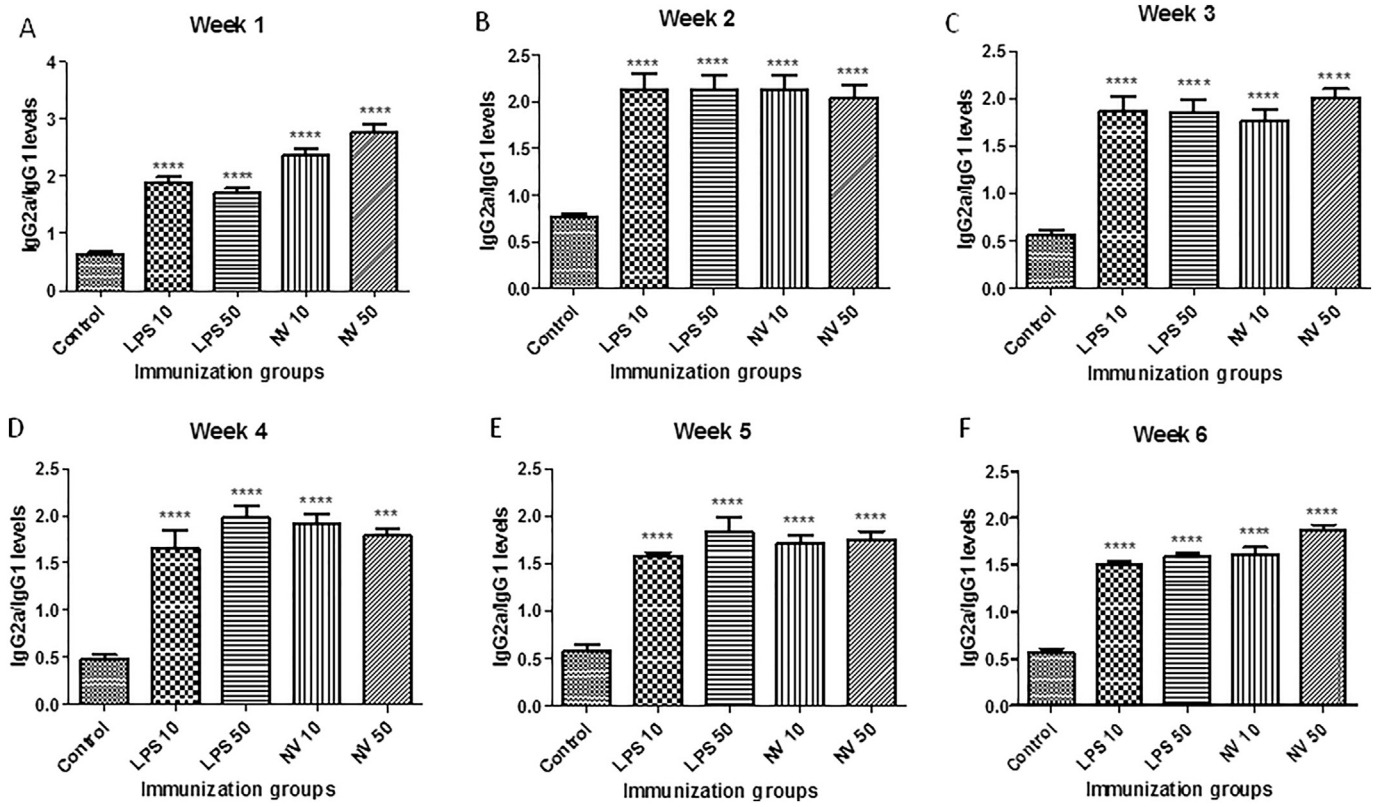

Fig. 9. IgG2a/IgG1 ratios in Balb/c mice at weeks 1, 2, 3, 4, 5, and 6. All the treatment groups showed IgG2a/IgG1 ratios > 1 for all of the 6 weeks post priming implying Th1 polarization, except the control group which demonstrated the genetic Th2 polarization in Balb/c mice as reported in literature. LPS 10 – LPS 10 μg and immunoadjuvant 100 μg; LPS 50 – LPS 50 μg and immunoadjuvant 100 μg; NV 10 – Nanovaccine with LPS 10 μg and immunoadjuvant 100 μg; NV 50 – Nanovaccine with LPS 50 μg and immunoadjuvant 100 μg. Values are expressed as mean ± SEM. *P* values: $^{*}P < .05$, $^{**}P < .01$, $^{***}P < .001$, $^{****}P < .0001$.

NV 50 exhibited more persistent immune stimulation that lasted up to 4 weeks post boosting. Interestingly, NV 10 too sustained high IgG levels up to 2 weeks post boosting. Thus, Balb/c mice nasally immunized with the nanovaccine formulations demonstrated activation of humoral immunity and a prolonged systemic immune response as well. Towards understanding the role of cell-mediated immunity (Th cells) and deducing the mechanism of immune activation, the levels of the IgG subclasses (IgG1 and IgG2a) were studied. With respect to IgG subclass switching, it is known that Th1/Th2 polarization is controlled by factors such as the genetic disposition of mice, the vaccine formulation per

se (Riquelme-Neira et al., 2013) and the immunization route. Balb/c mice are genetically polarized towards a Th2 response (Sislema-Egas et al., 2012; Choi et al., 2002), while many researchers have reported that *Brucella* vaccines promote switching towards a more dominant Th1 response both intranasally and parenterally in Balb/c mice. In this study, similar treatments were used for priming and booster immunizations, and it was observed that (i) the nanovaccine formulations induce a mixed Th1/Th2 type of immune response in Balb/c mice, (ii) nanovaccine formulations and antigen-immunoadjuvant solutions consistently switch the immune response to a dominant Th1 type, and (ii) Th1 dominance was observed from the first week post priming and therefore, the isotype switching is driven by the priming and not booster immunization. Mice primed by the nasal route developed higher *Brucella* specific IgG2a antibodies compared to IgG1 antibodies. Nasal priming induced therefore a stronger Th1 polarization, as already observed with other whole cell and sub-unit *Brucella* vaccine formulations (Finnegan et al., 1999; Coria et al., 2016; Kianmehr et al., 2015).

Local antigen-specific IgA and IgG antibodies were detected when mice were primed and boosted by the nasal route and clonal expansion of IgA signifying presence of activated effector plasma cells in the nasal mucosa. Interestingly, mucosal priming and boosting via nasal immunization triggered the systemic immune responses. In addition to the efficient mucosal priming, mice boosted by the nanovaccine NV 50 produced significant systemic IgG antibodies that were sustained up to four weeks. This implied that the slow antigen and immunoadjuvant release mechanism of the nanovaccine along with the nasal boost are indispensable for sustaining activation of plasma cells capable of homing to the MALT in the nasal tissues and releasing local and systemic immunoglobulins. Our data substantiate the significance of the booster immunization route to elicit a mucosal effector response. Thus, the nanovaccine designed using xyloglucan, acellular LPS, and an indigenous immunoadjuvant (quillaja saponin) demonstrated a positive sign of immune stimulation and probable protection against brucellosis.

5. Conclusion

In summary, *Brucella* specific mucosal and systemic immune responses were achieved by priming with the nanovaccine formulations and these responses could be efficiently boosted by the intranasal route. The route used for priming exhibited a mixed Th1/Th2 immune response and further, a stronger Th1 polarization in mucosally primed mice. The mice primed and/or boosted by the nasal route produced both cell-mediated and humoral immunity. The nanovaccine could sustain immunoglobulin levels for a prolonged period in vivo by virtue of its prolonged release properties and was found to be non-ciliotoxic and safe in rats. These results emphasize the significant role of priming in eliciting the quality and localization of the immune responses. Further, the nasal mucosal route poses as a prime-boost route for the coherent design of a lucrative vaccination strategy. Xyloglucan nanoparticles developed using RESS can as well be the new 'nanocarriers' for mucosal vaccines and can be adapted to develop vaccination strategies against many other infectious diseases.

Disclosure

The authors declares there is no conflict of interest.

Declaration of Competing Interest

The authors declare that they have no known competing financial interests or personal relationships that could have appeared to influence the work reported in this paper.

Acknowledgements

This work was supported by the Bill & Melinda Gates Foundation, USA [OPP124589].

The authors would like to thank Dr. Anuradha Majumdar, Bombay College of Pharmacy, India for in vivo studies.

Appendix A. Supplementary data

Supplementary data to this article can be found online at https://doi.org/10.1016/j.ijpx.2020.100053.

References

Avachat, A.M., Gujar, K.N., Wagh, K.V., 2013. Development and evaluation of tamarind seed xyloglucan-based mucoadhesive buccal films of rizatriptan benzoate. Carbohydr. Polym. 91, 537–542.
Barbi Mda, S., et al., 2015. Preparation and characterization of Chitosan Nanoparticles for Zidovudine Nasal Delivery. J. Nanosci. Nanotechnol. 15, 865–874.
Behboudi, S., Morein, B., Rönnberg, B., 1995. Isolation and quantification of Quillaja saponaria Molina saponins and lipids in iscom-matrix and iscoms. Vaccine 13 (17), 1690–1696. https://doi.org/10.1016/0264-410x(95)00107-c.
Bernocchi, B., Carpentier, R., Betbeder, D., 2017. Nasal nanovaccines. Int. J. Pharm. 530 (1–2), 128–138.
Bhalekar, M.R., Bargaje, R.V., Upadhaya, P.G., Madgulkar, A.R., Kshirsagar, S.J., 2016. Formulation of mucoadhesive gastric retentive drug delivery using thiolated xyloglucan. Carbohydr. Polym. 136, 537–542.
Brito, L.A., Singh, M., 2011. Acceptable levels of endotoxin in vaccine formulations during preclinical research. J. Pharm. Sci. 100, 34–37.
Choi, A.H., et al., 2002. The level of protection against rotavirus shedding in mice following immunization with a chimeric VP6 protein is dependent on the route and the coadministered adjuvant. Vaccine. 20, 1733–1740.
Ciabattini, A., Pettini, E., Arsenijevic, S., Pozzi, G., Medaglini, D., 2010. Intranasal immunization with vaccine vector Streptococcus gordonii elicits primed CD4+ and CD8+ T cells in the genital and intestinal tracts. Vaccine. 28, 1226–1233.
Cibulski, S.P., et al., 2016a. Quillaja brasiliensis saponins induce robust humoral and cellular responses in a bovine viral diarrhea virus vaccine in mice. Comp. Immunol. Microbiol. Infect. Dis. 45, 1–8.
Cibulski, S.P., et al., 2016b. Novel ISCOMs from Quillaja brasiliensis saponins induce mucosal and systemic antibody production, T-cell responses and improved antigen uptake. Vaccine. 34, 1162–1171.
Coria, L.M., et al., 2016. *Brucella abortus* Omp19 recombinant protein subcutaneously co-delivered with an antigen enhances antigen-specific T helper 1 memory responses and induces protection against parasite challenge. Vaccine. 34, 430–437.
Dorneles, E.M., Teixeira-Carvalho, A., Araujo, M.S., Sriranganathan, N., Lage, A.P., 2015. Immune response triggered by *Brucella abortus* following infection or vaccination. Vaccine. 33, 3659–3666.
Finnegan, A., Mikecz, K., Tao, P., Glant, T.T., 1999. Proteoglycan (aggrecan)-induced arthritis in BALB/c mice is a Th1-type disease regulated by Th2 cytokines. J. Immunol. 163, 5383–5390.
Fiorino, F., Pettini, E., Pozzi, G., Medaglini, D., Ciabattini, A., 2013. Prime-boost strategies in mucosal immunization affect local IgA production and the type of th response. Front. Immunol. 4 (128).
Goodwin, Z.I., Pascual, D.W., 2016. Brucellosis vaccines for livestock. Vet. Immunol. Immunopathol. 181, 51–58.
Hassan, A., Tang, Y.M., Ayres, J.W., 2004. Itraconazole formation using supercritical carbon dioxide. Drug Dev. Ind. Pharm. 30, 1029–1035.
Jiang, Y., Li, M., Zhang, Z., Gong, T., Sun, X., 2014. Enhancement of nasal HIV vaccination with adenoviral vector-based nanocomplexes using mucoadhesive and DC-targeting adjuvants. Pharm. Res. 31, 2748–2761.
Kaynak-Onurdag, F., Okten, S., Sen, B., 2016. Screening *Brucella* spp. in bovine raw milk by real-time quantitative PCR and conventional methods in a pilot region of vaccination, Edirne, Turkey. J. Dairy Sci. 99, 3351–3557.
Kianmehr, Z., Kaboudanian Ardestani, S., Soleimanjahi, H., Fotouhi, F., Alamian, S., Ahmadian, S., 2015. Comparison of biological and immunological characterization of lipopolysaccharides from *Brucella abortus* RB51 and S19. Jundishapur J. Microbiol. 8, e24853.
Li, Z.Q., et al., 2015. A *Brucella melitensis* M5-90 wboA deletion strain is attenuated and enhances vaccine efficacy. Mol. Immunol. 66, 276–283.
Lu, S., 2009. Heterologous prime-boost vaccination. Curr. Opin. Immunol. 21, 346–351.
Lycke, N., 2012. Recent progress in mucosal vaccine development: potential and limitations. Nat. Rev. Immunol. 12, 592–605.
Mahomed, H., et al., 2013. TB incidence in an adolescent cohort in South Africa. PLoS One 8, e59652.
Martins Rda, C., Irache, J.M., Gamazo, C., 2012. Acellular vaccines for ovine brucellosis: a safer alternative against a worldwide disease. Expert Rev. Vaccines. 11, 87–95.
Mathaes, R., Winter, G., Besheer, A., Engert, J., 2014. Influence of particle geometry and PEGylation on phagocytosis of particulate carriers. Int. J. Pharm. 465, 159–164.
Medaglini, D., et al., 2006. In vivo activation of naive CD4+ T cells in nasal mucosa-associated lymphoid tissue following intranasal immunization with recombinant Streptococcus gordonii. Infect. Immun. 74, 2760–2766.

Moon, J.J., Huang, B., Irvine, D.J., 2012. Engineering nano-and microparticles to tune immunity. Adv. Mater. 24 (28), 3724–3746.
Moreno, E., 2014. Retrospective and prospective perspectives on zoonotic brucellosis. Front. Microbiol. 5 (213).
Mullers, K.C., Paisana, M., Wahl, M.A., 2015. Simultaneous formation and micronization of pharmaceutical cocrystals by rapid expansion of supercritical solutions (RESS). Pharm. Res. 32, 702–713.
Mumtaz, A.H., Ching, H., 1995. Design of a dissolution apparatus suitable for in-situ release study of triamicinolone acetonide from bioadhesive buccal tablets. Int. J. Pharm. 121, 129–139.
Neutra, M.R., Kozlowski, P.A., 2006. Mucosal vaccines: the promise and the challenge. Nat. Rev. Immunol. 6, 148–158.
Otero-Pareja, M.J., Casas, L., Fernandez-Ponce, M.T., Mantell, C., Martinez de la Ossa, E.J., 2015. Green extraction of antioxidants from different varieties of red grape pomace. Molecules. 20, 9686–9702.
Padmajan Sasikala, S., Poulin, P., Aymonier, C., 2016. Prospects of supercritical fluids in realizing graphene-based functional materials. Adv. Mater. 28, 2663–2691.
Pakzad, I., Rezaee, A., Rasaee, M.J., Hossieni, A.Z., Tabbaraee, B., Kazemnejad, A., 2010. Protection of BALB/C mice against *Brucella abortus* 544 challenge by vaccination with combination of recombinant human serum albumin-l7/l12 (*Brucella abortus* ribosomal protein) and lipopolysaccharide. Roum. Arch. Microbiol. Immunol. 69, 5–12.
Pettini, E., Ciabattini, A., Pozzi, G., Medaglini, D., 2009. Adoptive transfer of transgenic T cells to study mucosal adjuvants. Methods. 49, 340–345.
Radosevic, K., Rodriguez, A., Lemckert, A., Goudsmit, J., 2009. Heterologous prime-boost vaccinations for poverty-related diseases: advantages and future prospects. Expert Rev. Vaccines. 8, 577–592.
Riquelme-Neira, R., et al., 2013. A. Protective effect of a DNA vaccine containing an open reading frame with homology to an ABC-type transporter present in the genomic island 3 of *Brucella abortus* in BALB/c mice. Vaccine. 31, 3663–3667.
Rowland, R., McShane, H., 2011. Tuberculosis vaccines in clinical trials. Expert Rev. Vaccines. 10, 645–658.
Rowland, R., et al., 2013. Safety and immunogenicity of an FP9-vectored candidate tuberculosis vaccine (FP85A), alone and with candidate vaccine MVA85A in BCG-vaccinated healthy adults: a phase I clinical trial. Hum. Vaccin. Immunother. 9, 50–62.
Shakya, A.K., Chowdhury, M.Y., Tao, W., Gill, H.S., 2016. Mucosal vaccine delivery: current state and a pediatric perspective. J. Control. Release 240, 394–413.
Sislema-Egas, F., Cespedes, S., Fernandez, P., Retamal-Diaz, A., Saez, D., Onate, A., 2012. Evaluation of protective effect of DNA vaccines encoding the BAB1_0263 and BAB1_0278 open reading frames of *Brucella abortus* in BALB/c mice. Vaccine. 30, 7286–7291.
Sotnikov, D.V., et al., 2015. Express immunochromatographic detection of antibodies against *Brucella abortus* in cattle sera based on quantitative photometric registration and modulated cut-off level. J. Immunoass. Immunochem. 36, 80–90.
Wang, Z., Wu, Q., 2013. Research progress in live attenuated *Brucella* vaccine development. Curr. Pharm. Biotechnol. 14, 887–896.
Wang, X., et al., 2014. Effects of partial deletion of the wzm and wzt genes on lipopolysaccharide synthesis and virulence of *Brucella abortus* S19. Mol. Med. Rep. 9, 2521–2527.
Wang, J.S., Wai, C.M., Brown, G.J., Apt, S.D., 2016. Two-dimensional nanoparticle cluster formation in supercritical fluid CO2. Langmuir. 32, 4635–4642.
Warren, H.S., Glennon, M.L., Wainwright, N., Amato, S.F., Black, K.M., Kirsch, S.J., Riveau, G.R., Whyte, R.I., Zapol, W.M., Novitsky, T.J., 1992. Binding and neutralization of endotoxin by Limulus antilipopolysaccharide factor. Infect Immun 60, 2506–2513.
Wong, J.P., Cherwonogrodzky, J.W., Di Ninno, V.L., Stadnyk, L.L., Knodel, M.H., 1992. Liposome potentiation of humoral immune response to lipopolysaccharide and O-polysaccharide antigens of *Brucella abortus*. Immunology. 77, 123–128.
Yen, C.H., Lin, H.W., Phan, T.D., Tan, C.S., 2011. Chemical fluid deposition of monometallic and bimetallic nanoparticles on ordered mesoporous silica as hydrogenation catalysts. J. Nanosci. Nanotechnol. 11, 2465–2469.
Zuercher, A.W., 2003. Upper respiratory tract immunity. Viral Immunol. 16, 279–289.